Generalized factorization and resummation

C. Balázs, J.C. Collins, D.E. Soper

Abstract

In this section we summarize the formalism which extends the usual hadronic factorization theorem to the low transverse momentum region for the inclusive production of colorless final states, while resumming logarithms with the ratio of the invariant mass and transverse momentum. Among the various recent applications the calculation of the Z^0 and Higgs boson transverse momentum distributions are highlighted.

1 The Collins-Soper-Sterman formalism

The standard factorization formula fails near kinematic boundaries. We discuss the case of low transverse momentum in Z_0 production, etc; this is an important case because the cross section peaks there. The failure of the factorization formula is symptomized by large corrections involving a factor of $\ln^2 Q/Q_T$ for each power of α_s.

Although the solutions to the problem are all commonly referred to as "resummations", there are in fact two very different approaches. One is resummation in its strict sense: One performs a selective and approximation summation of the largest parts of the perturbative series for the hard scattering in the standard factorization formalism.

The second approach is that of Collins, Soper and Sterman (CSS) [1, 2, 3]. These authors observed that the conventional factorization formalism is in fact wrong at low transverse momentum and they derive a correct factorization for this region. In an intermediate region of transverse momentum, the standard factorization with resummation is applicable with somewhat reduced accuracy, and there is an overlap between the two approaches, which we will discuss later.

In any case, it is essential to improve on the standard fixed-order factorization formalism, and the reward is an improved method that

- includes large, logarithmic QCD corrections up to all orders in the strong coupling,
- improves the renormalization scale dependence of the prediction,
- enables prediction of certain quantities reliably, which cannot be done in a fixed order calculation,
- provides an independent, analytic check for parton shower Monte Carlo's.

1.1 k_T-dependent parton densities

CSS realized that the failure of the standard factorization when $Q_T \ll Q$ occurs because it neglects the transverse motion of the incoming partons in the hard scattering. (Here Q can be the invariant mass of a colorless particle, or set of particles, created in a hard partonic collision, and Q_T is the related transverse momentum.) The approximation of neglecting parton transverse momentum is only valid when the cross section is integrated over a large range of Q_T. But if, for example, Q_T is of order 1 GeV, then we are outside of the domain in which the factorization is applicable.

A fully satisfactory approach must use a factorization theorem that is valid for any Q_T that is small compared to Q. CSS's theorem gives the cross section as a convolution of transverse momentum distributions

$$\frac{d\sigma}{d^4Q} \propto \int d^2k_T P(x_1, k_T) P(x_2, Q_T - k_T), \tag{1}$$

where P is a partonic density distribution that is a function of both longitudinal (x) and transverse (k_T) momenta. The partonic recoil against soft gluons as well as the intrinsic partonic transverse momentum are included in P.

Such a treatment completely formalizes the intuitive notion that partons must have transverse momentum and that this transverse momentum gives rise to transverse momentum of the Drell-Yan pair. There is then no need to convolute a calculated cross section with "intrinsic transverse momentum" for the quarks; this manoeuvre is only necessary as an ad hoc correction to a formalism that is incomplete.

In QCD, complications arise from soft-gluon effects, because these effects do not cancel, in contrast to the case of the cross section integrated over Q_T. A consequence, proved by CSS, is a particular form of the evolution equations for the k_T-dependent parton densities. These equations are *not* the normal DGLAP equations[1]. The kernel of the evolution contains a perturbatively calculable part and non-perturbative part. The non-perturbative part can be summarized by saying that there is a fixed amount of gluon radiation per *unit rapidity*, so that the transverse momentum distribution of the partons broadens in a characteristic way with energy. The non-perturbative part of this energy-dependent radiation is fitted by the g_2 term of Eq.(10) below.

This feature may be the dominant reason why transverse momentum distributions are so broad at high energies, as in Z^0 production: the transverse momentum of the Z^0 has a component due to the recoil against non-perturbative glue emitted into many units of rapidity.

The CSS formalism clearly entails a phenomenological fitting of the non-perturbative part of the k_T-dependent parton densities and the evolution kernel. In principle, this can be done at fairly low energy, and then the evolution equations predict the results for higher energies with no further adjustable parameters. The more conventional resummation formalism is compatible with the CSS formalism, but it is not as complete.

[1] Although all the physics associated with the DGLAP equations is present.

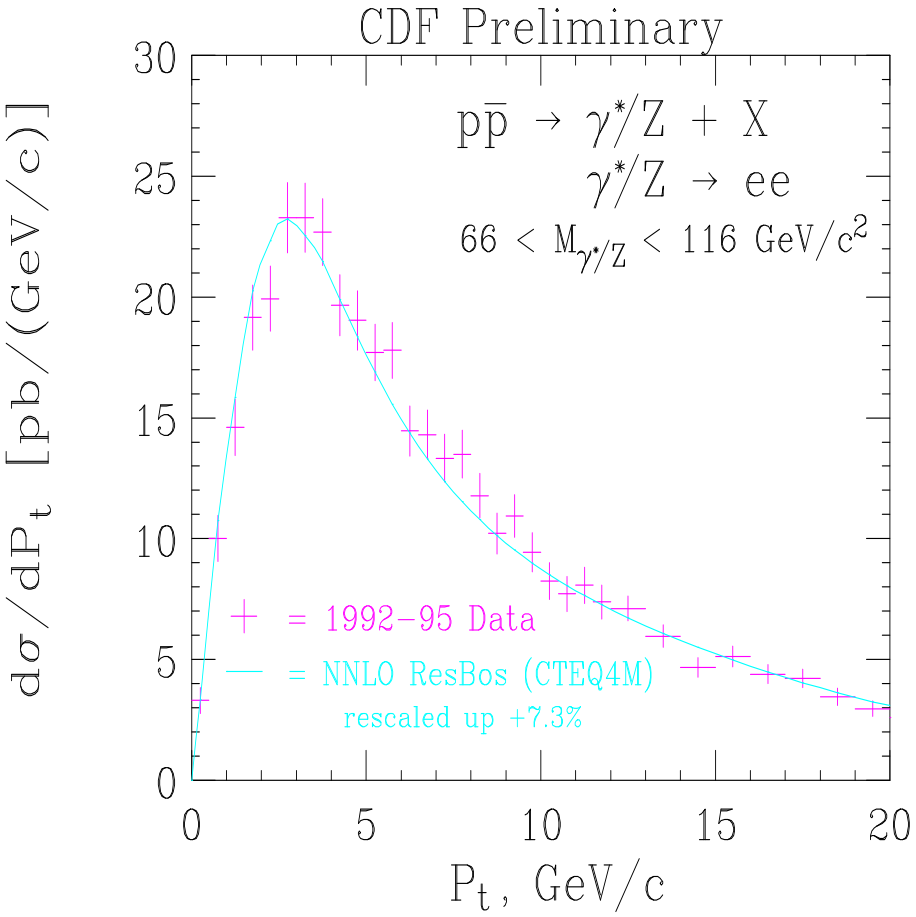

Figure 1: Transverse momentum distribution of electron-positron pairs from decays of (mostly) Z^0 bosons, produced at the Tevatron in $\sqrt{S} = 1.8$ GeV center of mass proton–anti-proton collisions. The data are CDF preliminary [4], and the curve is calculated by the ResBos Monte Carlo event generator [5, 6].

Because the CSS formalism is designed to treat correctly the $Q_T \ll Q$ region, it also provides an appropriate resummation of the large logarithms, $\ln(Q/Q_T)$ in the standard factorization formula.

We can gauge how important these logarithms are in practice by examining the cross section for Z production at the Tevatron. The bulk of the cross section is in the low Q_T region, and, as can be seen from Fig. 1, there is a peak at around $Q_T = 2.7$ GeV, which is much smaller than the invariant mass $Q = m_Z = 91.187$ GeV. This implies that for the bulk of the events $\ln(Q/Q_T)$ is large enough that $\alpha_s(m_Z)\ln^2(Q/Q_T) > 1$. Since we have a double logarithm for each radiated gluon, higher orders in the perturbative series are not suppressed.

1.2 From fixed order to resummed

In this section we show how the results of the standard factorization theorem are related to a resummation in terms of leading logarithms, etc.

When the Z^0 is produced in a hadron-hadron collision its transverse momentum is balanced by some hadronic activity which stems from partons emitted by the initial state partons. (In the first order in the strong coupling a Z^0 and a gluon is produced.) The Q_T distribution given by the usual factorization in the low Q_T region is written as

$$\lim_{Q_T\to 0}\frac{d\sigma}{dQ_T^2} = \sum_{n=1}^{\infty}\sum_{m=0}^{2n-1}\alpha_s^n\ {}_nv_m\ \ln^m\left(\frac{Q^2}{Q_T^2}\right) + \mathcal{O}\left(\frac{1}{Q_T}\right), \tag{2}$$

where the coefficients ${}_nv_m$ are perturbatively calculable apart from some factors of parton densities. When the two scales Q and Q_T are very different, the logarithmic terms $\ln^m(Q^2/Q_T^2)$ are large, and for $Q_T \ll Q$ the perturbative series is dominated by these terms. For $Q_T \ll Q$ truncation of the perturbative series, i.e. any fixed order calculation, gives an answer which neglects these important all order logarithmic contributions. At the lowest order, $\mathcal{O}(\alpha_s^0)$, the Z^0 boson is produced alone, that is with a Q_T distribution of $\delta(Q_T)$. The singularity at $Q_T = 0$ prevails at any fixed order in α_s, as Eq. (2) shows.

One way of reorganizing the perturbation series is to make the expansion one in terms of $\alpha_s\ln^2(Q/Q_T)$ instead of α_s itself. In this simplified picture, calculating fixed order QCD corrections means calculating the perturbative series

$$\begin{aligned}\lim_{Q_T\to 0}\frac{d\sigma}{dQ_T^2} = \\ Q_T^{-2}\Big\{&\alpha_s({}_1v_1'L + {}_1v_0') + \alpha_s^2({}_2v_3'L^3 + {}_2v_2'L^2) + \alpha_s^3({}_3v_5'L^5 + {}_3v_4'L^4) + \ \ldots \\ &+ \alpha_s^2({}_2v_1'L_2 + {}_2v_0'L^0) + \alpha_s^3({}_3v_3'L^3 + {}_3v_2'L^2) + \ \ldots \\ &+ \ \ldots \qquad\qquad \ldots\Big\},\end{aligned}$$

column by column. In the leading logarithm approach, on the other hand, we calculate the above series line by line [7]. While in the fixed order (column by column) calculation the convergence for low Q_T is spoiled by the higher order uncalculated logs ($L = \ln(Q/Q_T)$), in the resummed (line by line) calculation convergence is preserved in each "order" (by each line), and higher order corrections are systematically included.

1.3 The CSS formula

The improved factorization theorem of CSS together with their evolution equation for the k_T dependent parton distributions, leads [3] to a useful formula[2] for the cross section. For Z^0 production it can be written as

$$\frac{d\sigma(h_1 h_2 \to Z^0 X)}{dQ^2\, dQ_T^2\, dy} = \sum_j \sigma_{0,j} W_{j\bar{j}}(Q, Q_T, x_1, x_2) \; + \; Y(Q, Q_T, x_1, x_2), \tag{3}$$

where the "resummed" part, $W(Q, Q_T, x_1, x_2)$, is defined as

$$\begin{aligned} W_{j\bar{j}}(Q, Q_T, x_1, x_2) \;\; &= \\ &\frac{1}{(2\pi)^2} \int d^2b\, e^{i\vec{Q}_T \cdot \vec{b}}\, \mathcal{C}_{j/h_1}(Q, b, x_1, \mu) e^{-\mathcal{S}(Q, b_*)} \mathcal{C}_{\bar{j}/h_2}(Q, b, x_2, \mu) \end{aligned} \tag{4}$$

for a given partonic initial state with flavor j.[3] The Fourier integral is introduced because transverse momentum conservation is explicit in the impact parameter, b, space [8].

All the dangerous logarithms are included in the perturbative Sudakov exponent

$$\mathcal{S}(Q, b_*) = \int_{C_0^2/b_*^2}^{Q^2} \frac{d\overline{\mu}^2}{\overline{\mu}^2} \left[A\left(\alpha_s(\overline{\mu})\right) \ln\left(\frac{Q^2}{\overline{\mu}^2}\right) + B\left(\alpha_s(\overline{\mu})\right) \right]. \tag{5}$$

Here C_0 is an arbitrary parameter which cuts off the perturbative low Q_T region.[4] To prevent perturbative calculations from being done in region where perturbation theory is inapplicable, the "impact parameter" b in the Sudakov exponent was replaced by

$$b_* = \frac{b}{\sqrt{1 + (b/b_{\max})^2}}. \tag{6}$$

The errors caused by this replacement are of the same form as the non-perturbative contributions to be discussed below, and are therefore correctly treated by being absorbed into the non-perturbative part of the formula.

The A and B functions are free of large logarithms and can be reliably calculated perturbatively for a given process as

$$A\left(\alpha_s(\bar{\mu})\right) = \sum_{n=1}^{\infty} \left(\frac{\alpha_s(\bar{\mu})}{\pi}\right)^n A^{(n)}, \quad B\left(\alpha_s(\bar{\mu})\right) = \sum_{n=1}^{\infty} \left(\frac{\alpha_s(\bar{\mu})}{\pi}\right)^n B^{(n)}. \tag{7}$$

[2] While solving the RGE, an integro-differential equation, specific choices of integration constants were made (c.f. Ref. [3]): $C_1 = C_3 = 2e^{-\gamma_E} \equiv C_0$ and $C_2 = C_4 = 1$, to optimize logarithmic contributions. This is similar to the $\mu = Q$ choice in case of the ultraviolet renormalization, to make terms like $\ln(\mu/Q)$ vanish.

[3] The lowest order partonic total cross section is $\sigma_{0,j} = \pi^2 g^2((1 - 4Q_j s_w^2)^2 - 1)/(48Q^2 c_w^2)$, where g is the weak coupling constant, s_w^2 (c_w^2) is the sine (cosine) of the weak mixing angle squared, and Q_j is the charge of the quark flavor j.

[4] In practice $C_0 = 2e^{-\gamma_E}$ is used, which is related to the values of the integration constants of the RGE for the k_T dependent PDF's.

The distributions

$$\mathcal{C}_{j/h}(Q,b,x,\mu) = \sum_a \int_x^1 \frac{d\xi}{\xi} C_{ja}\left(b_*, \frac{x}{\xi}, \mu\right) f_{a/h}(\xi,\mu)\, \mathcal{F}_{a/h}(b,x)\, e^{-r(b)\ln Q} \tag{8}$$

depend on virtual and real emission contributions for a given process, via the Wilson coefficients C_{ja}. Just as the A and B functions the Wilson coefficients are expanded in terms of the strong coupling α_s

$$C_{ij}\left(b_*, z, \mu\right) = \sum_{n=0}^{\infty} \left(\frac{\alpha_s(\mu)}{\pi}\right)^n C_{ij}^{(n)}\left(z, b_*\right). \tag{9}$$

Since the Sudakov exponent integrates to unity, the C_{ij} function sets the normalization of the resummed distribution. In particular, if coefficients up to $C_{ij}^{(n)}$ are included in the calculation then the resummed rate will equal the rate calculated in fixed order at $\mathcal{O}(\alpha_s^n)$ [5]. The function $f_{a/h}(x,\mu)$ is the usual renormalized momentum fraction (x) distribution of parton a in hadron h at the energy scale μ. Observe that the impact parameter dependence of the perturbative coefficient functions is cut off by the use of b_* instead of b.

Included in Eq. (8) are two non-perturbative factors, $\mathcal{F}_{a/h}(b,x)$ and $e^{-r(b)\ln Q}$. These implement the parts of the CSS factorization and evolution equation that cannot be implemented as a resummation of the standard factorization theorem. They also compensate for the errors in the resummation at large b. The overall effect is that (8) define k_T-dependent parton densities. The $\mathcal{F}$ factor can be interpreted as allowing for intrinsic transverse momentum, and the $e^{-r(b)\ln Q}$ factor allows for the recoil against soft gluon radiation. The $\ln Q$ in the exponent of the soft-gluon factor comes from the solution of the CSS evolution equation and can be interpreted by saying that soft gluons are emitted uniformly in rapidity.

The perturbative part of the formula uses b_* instead of b, as defined by Eq. (6). The parameter $b_{\max}$ provides an infra-red cutoff on the perturbative part of the formula. In practice the empirically optimal value, $b_{\max} = 1/2\ \mathrm{GeV}^{-1}$, is used. This arbitrary cutoff of the b integration is compensated by the parameterization of the non-perturbative part of the formula, which is

$$\begin{aligned} W_{ij}^{\mathrm{NP}}(Q,b,x_1,x_2) &= \mathcal{F}_{i/h_1}(Q,b,x_1)\mathcal{F}_{j/h_2}(Q,b,x_2)e^{-r(b)\ln Q} \\ &= \exp\left[-g_1 b^2 - g_2 b^2 \ln\left(\frac{Q}{2Q_0}\right) - g_1 g_3 b \ln\left(100 x_1 x_2\right)\right], \end{aligned} \tag{10}$$

where Q_0 is chosen to be the initial scale of the parton evolution[5] and the g_i parameters have to be determined using experimental data.[6]

1.4 Matching

The resummed term, defined by Eq. (4), was derived in the context of a generalized factorization, under the assumption that $Q_T \ll Q$. This assumption will break down within

[5]For recent CTEQ PDF's $Q_0 = 1.6$ GeV.

[6]The $\ln\left(Q^2/Q_0^2\right)$ term is introduced to match the logarithmic term of the Sudakov exponent and its coefficient is expected to be process independent, depending only on the initial partonic state.

and beyond the intermediate $Q_T \lesssim Q$ region. In the high Q_T region (where $Q_T \gtrsim Q$) the conventional perturbative factorization formalism is reliable. To obtain sufficiently accurate results for all Q_T, it is necessary to combine the formalisms.

The Y term in Eq. (3) was introduced by CSS [2] to correct the behavior of the resummed piece in the intermediate and high Q_T regions.[7] It is defined as the difference of the cross section calculated from the standard factorization formula at a fixed order n of perturbation theory and the $Q_T \ll Q$ asymptote of this cross section:

$$Y(Q, Q_T, x_1, x_2) = \left(\frac{d\sigma}{dQ^2\, dQ_T^2 dy}\right)_n - \left(\frac{d\sigma}{dQ^2\, dQ_T^2 dy}\right)_{n, Q_T \ll Q}. \tag{11}$$

Thus, the full CSS formula can be written as

$$\frac{d\sigma}{dQ^2\, dQ_T^2 dy} = \left(\frac{d\sigma}{dQ^2\, dQ_T^2 dy}\right)_{\rm res} + \left(\frac{d\sigma}{dQ^2\, dQ_T^2 dy}\right)_n - \left(\frac{d\sigma}{dQ^2\, dQ_T^2 dy}\right)_{n, Q_T \ll Q}. \tag{12}$$

This method of matching the resummed and fixed order pieces is valid because the low Q_T asymptote used in Eq. (11) is the same as the large Q_T asymptote of the resummed term W. At low Q_T the asymptotic part dominates the Q_T distribution (the logs are large), and the last two terms cancel in Eq.(12), while the resummed term is significant near $Q_T = 0$. At high Q_T the logs are small, and the expansion of the resummed term cancels the Q_T singular terms up to higher orders in α_s.[8] In this situation the first and third terms cancel and CSS formula reduces to the fixed order perturbative result. After matching the resummed and fixed order cross sections in such a "smooth" manner, it is expected that the normalization of the CSS cross section reproduces the fixed order total rate, since when expanded and integrated over Q_T it deviates from the fixed order result only in small higher order terms in α_s [5].

Unfortunately the above argument does not completely work in practice. The problem arises because at large Q_T the W term in Eq. (3) is an extrapolation of the cross section from small Q_T. So it has a $1/Q_T^2$ behavior, modified by logarithms. This falls less steeply than the true cross section, which is subject to kinematic limits. The errors in the CSS formula at large Q_T are indeed suppressed by a power of α_s. But the coefficient of this power is the $1/Q_T^2$ part of the formula, and so the error can be easily larger than the true cross section. A symptom of the problem is that the cross section calculated from Eq. (3) is typically negative at large enough Q_T.

One possible remedy [9] is to abandon the CSS formalism. But we regard this as undesirable, because it also abandons the important physical result of CSS that goes beyond mere resummation: their proper treatment of non-perturbative transverse momentum.

A second, commonly used remedy, is to utilize the fact that in the high Q_T region the fixed order result is a good description of the distribution. So when calculating the Q_T distribution one can simply switch from the CSS to the fixed order distribution whenever they cross for high Q_T's. Since the mismatch between the resummed and the asymptotic

[7] The exact definition of the Y piece for Z^0 production can be found in Refs. [3, 5].

[8] The cancellation is higher order than the order at which the singular pieces were calculated.

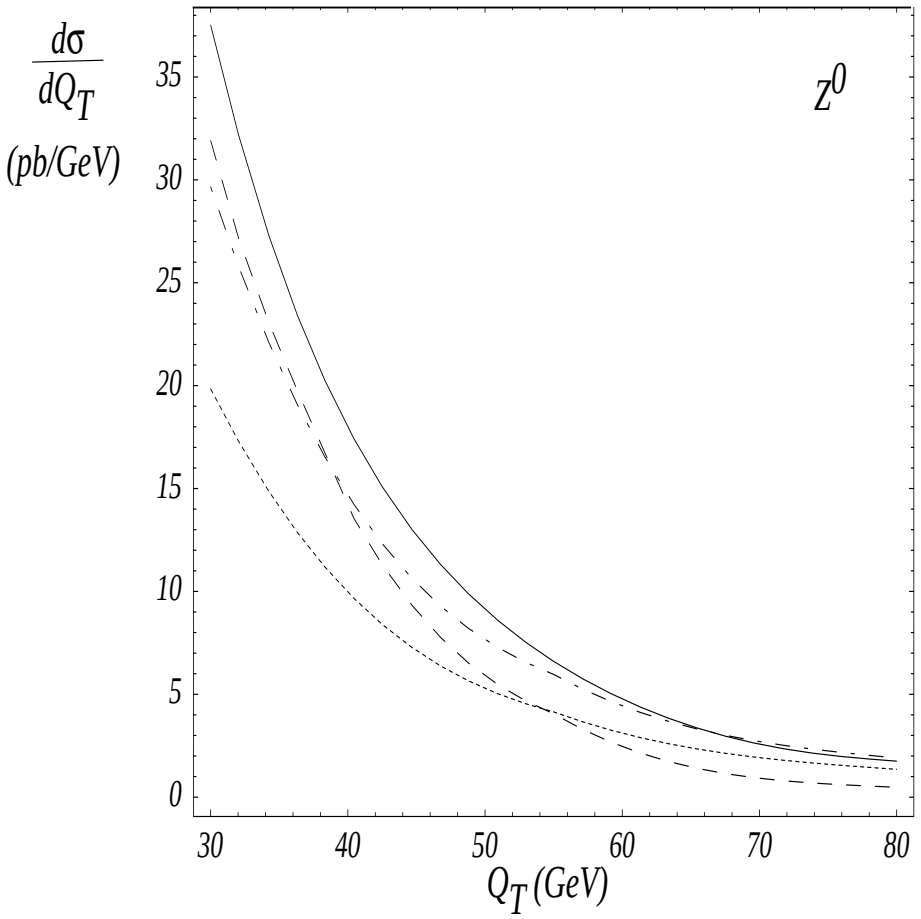

Figure 2: Transverse momentum distributions calculated using the CSS (solid and dashed) and the usual factorization (dot-dashed and dotted) formalisms. The CSS calculation is not switched over to the usual formalism to show the typical "kink" which occurs at a switching point. The solid and dot-dashed curves are calculated at $\mathcal{O}(\alpha_s^2)$, while the dashed and dotted curves are at $\mathcal{O}(\alpha_s)$, illustrating the improvement of the high Q_T behavior of the CSS formula with the perturbative order.

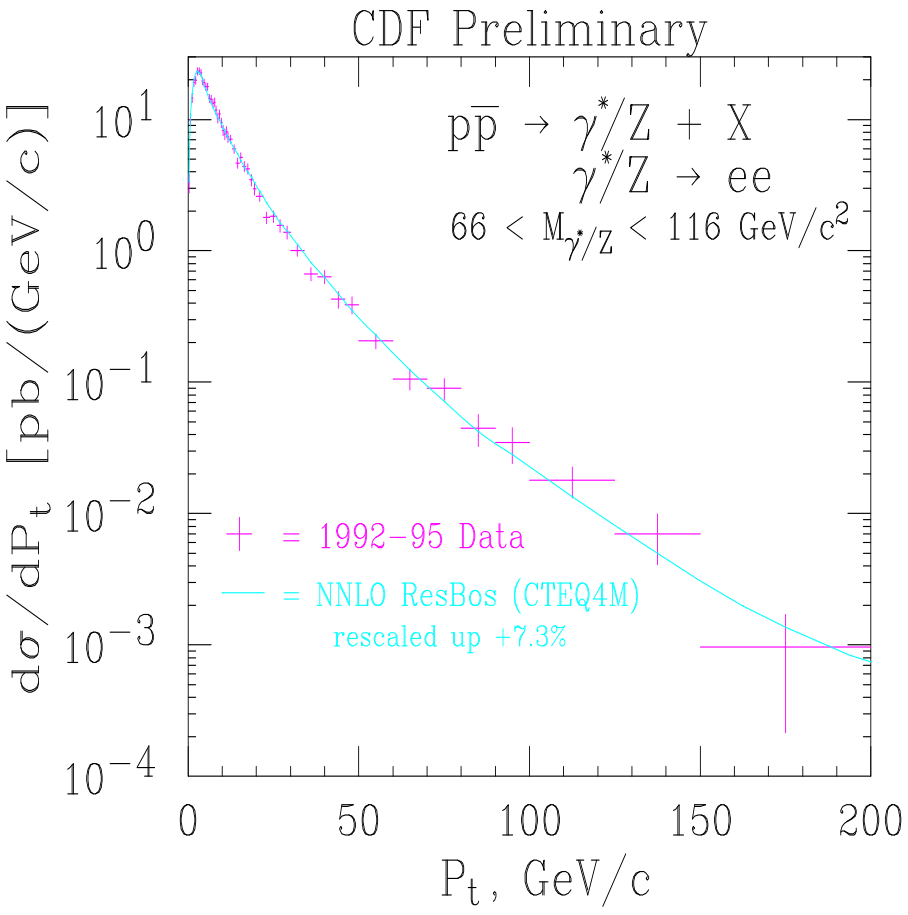

Figure 3: Same as Fig. 1, except shown for the full range of transverse momentum Q_T. Switching from the CSS to the usual factorization formalism in the $60 \lesssim Q_T \lesssim 70$ GeV region (c.f. [5]), results in a smooth Q_T distribution which agrees well with the experiment in the full Q_T range.

terms in Eq.(12) decreases as the perturbative order of the calculation (n) increases, it is expected that the crossing point shifts toward $Q_T = Q$, and the slope of the resummed and fixed order curves approaches each other as n increases (cf. Ref. [5]). Indeed, calculations at $\mathcal{O}(\alpha_s^2)$ blend closer to m_Z, and smoother than at $\mathcal{O}(\alpha_s)$, as shown in Fig. 2.

When this prescription for the switching is followed at the fully differential, $d\sigma/dQ_T dQ dy$, level the result is a smooth and differentiable Q_T distribution, after the invariant mass and rapidity is integrated out. This is illustrated in Fig. 27. It was shown in Ref. [5] that the integral of the Q_T distribution calculated using this prescription recovers the fixed order total rate within an error which is the size of the higher orders, as it is expected.

1.5 Improved matching

Since the calculations of W and Y are done using truncations of perturbation theory, the switching between calculational methods introduces an artificial discontinuity in the slope of the cross section. This practical problem arises in the matching because of a mismatch of the orders of perturbation theory at which W and Y are calculated. From the point of view of a standard factorization calculation, W contains a selective summation of arbitrarily high orders of perturbation theory. The possibility of getting such a resummation relies on performing certain approximations that are only valid at small Q_T. The difficulty of performing complete higher-order calculation means that Y can only be calculated at fixed order.

At large transverse momentum, $|W|$ is much larger than the actual cross section, and so the cross section Eq. (12) is obtained by the cancellation of two almost equal terms. This is clearly a recipe for bad numerical work.

Examination of the lowest-order calculation of Y, for the $q\bar{q}$ annihilation term [2] shows some of the sources of the problems:

$$\begin{aligned} Y \;=\; & \frac{C}{Q_T^2}\int \frac{d\xi_1}{\xi_1}\frac{d\xi_2}{\xi_2} f_q(\xi_1) f_{\bar{q}}(\xi_2) \\ & \left\{ \frac{(Q^2-\hat{t})^2+(Q^2-\hat{u})^2}{\hat{s}}\delta(\hat{s}+\hat{t}+\hat{u}-Q^2) \right. \\ & -2\delta(1-x_1/\xi_1)\delta(1-x_2/\xi_2)\left[\ln(Q^2/Q_T^2)-\frac{3}{2}\right] \\ & \left. -\delta(1-x_1/\xi_1)\left[\frac{1+x_2^2/\xi_2^2}{1-x_2/\xi_2}\right]_+ - \left[\frac{1+x_1^2/\xi_1^2}{1-x_1/\xi_1}\right]_+ \delta(1-x_2/\xi_2)\right\}. \end{aligned} \tag{13}$$

Here x_1 and x_2 are the longitudinal momentum fractions of the Drell-Yan pair. The first term contains the usual perturbative calculation of the differential cross section, and the other 3 terms give the negative of its low Q_T asymptote. The intrinsic rate of fall off of the cross section with Q_T is given by the explicit $1/Q_T^2$ factor which is present in the parton cross section. But an extra fall off is caused by the fact that the parton densities are probed at larger fractional momenta when Q_T is increased.

Some symptoms of the problems can already be seen. One is that the first subtraction term, on the second line of Eq. (13), changes sign at large Q_T: the extrapolation of a positive

cross section becomes negative. The second is the plus distribution in the third line; if the parton distributions are steeply falling, the plus distributions give a misleading size for the integrand. This last effect really indicates that there is an additional scale in the process, so that the relevant scales are:

- The transverse momentum Q_T of the Drell-Yan pair.
- The invariant mass Q of the pair.
- The increase ΔQ of Q that is necessary to make the typical parton densities in the factorization formula decrease by a factor 2.

We believe the overall approach of a subtraction method is correct: W correctly represents the physics at low Q_T, and we do not wish to give up a method that uses the intuitive notion of k_T-dependent parton densities. We therefore cannot expect to obtain a perfect estimate of the large Q_T cross section from W alone. The idea of adding a correction term Y is a good way of combining the information in standard fixed order calculations with the resummed calculations.

But improvements in its implementation are needed. We suggest the following strategies that could be tried, individually or even in combination:

- Multiply W by an ad hoc factor $F(Q_T/M)$. Correspondingly the formula for the subtraction term in Y will also have the same factor. The parameter M is in principle arbitrary, and it should be chosen so that the fall off in the modified W term mimics that of the actual cross section. The cut-off function obeys $F(0) = 1$, so that the small Q_T behavior is unchanged, and the function should be zero for large Q_T.
- Change the argument of W from Q_T to some other function of Q_T. One possible choice would be $Q'_T = Q_T/(1 - Q_T/M)$, where M is again a parameter to be chosen. One would replace W by zero if $Q_T > M$. The effect of the variable change is to leave W unaltered at small Q_T and to give a more rapid fall off at large Q_T. Again one would make an identical redefinition in the subtraction term in Y.
- Redefine the + distributions such as those in Eq. (13), by:

$$\int_0^1 dz f(z) \left[\frac{1}{z}\right]_{+,z_0} = \int_0^1 dz \frac{1}{z} \left[f(z) - f(0)\theta(z_0 - z)\right]. \tag{14}$$

  (The usual definition has $z_0 = 1$.)

In each case we have a generalized renormalization-group invariance of the exact cross section under changes of the parameter M or z_0. But approximations obtained by truncation of a perturbation series are invariant only up to a term of order the first uncalculated correction. The aim is to choose the parameters on physical grounds to be such as to keep these higher order terms small, to eliminate their reason(s) for being large.

1.6 Applications

Beyond Z^0 production, in its present form, the CSS formalism can be applied in hadron-hadron collisions whenever the final state is colorless. The phenomenological significance of this "transverse momentum resummation" ranges from Drell-Yan pair production, through lepton pair production via $W^{\pm}$ and Z^0 bosons [5], di-gauge boson (e.g. photon or Z^0 boson pair) production [10, 11], to Higgs production [12, 13, 14]. In recent years it was tested in hadronic processes taking place at fixed target (e.g. in DY photon and diphoton production) [15] and collider energies (e.g. in DY, $W^{\pm}$, Z^0, and diphoton production). It was applied for different hadronic initial states in pion–nucleon, proton–nucleon, and proton–anti-proton collisions. It was also modified and tested for DIS processes [16]. Finally, since was first devised for the calculation of the energy correlation of jets in e^+e^- collisions [1], it can be used in jet production at lepton colliders. Such a wide variety of applicability, and good agreement with existing experimental results for different processes, colliders, center of mass energies, and initial states gives us a confidence in the resummed predictions for the LHC.

2 Higgs production

At the LHC the SM Higgs boson will be mainly produced through the gluon fusion subprocess via a top quark loop: gg (top quark loop) $\rightarrow HX$ [17]. The Higgs boson can be detected in its $H \rightarrow \gamma\gamma$ decay mode, if its mass is in the 100-150 GeV range [18]. If the Higgs mass is higher than about 130 GeV then its $H \rightarrow Z^0 Z^{0*}$ decay mode is the cleanest and most significant [18]. To distinguish these signals from the substantial QCD background, besides the sharp peak in the invariant mass distribution, the most straightforward measurable to use is the transverse momentum. According to earlier studies, a statistical significance on the order of 5-10 can be reached for the inclusive $H \rightarrow \gamma\gamma$ signal, actual values depending on luminosity and background estimates. Once their transverse momentum distribution is reliably predicted, the difference in the Q_T of the signal and background can be utilized to devise kinematic cuts to enhance the statistical significance of the signal. After the discovery, when determining the properties of the Higgs boson, besides the total cross section and the invariant mass distribution, the simplest and most fundamental measurable to use is the transverse momentum. For a recently proposed new detection mode, $H \rightarrow \gamma\gamma$jet, in Ref. [19] it was also found that in order to optimize the significance it is necessary to impose a 30 GeV cut on the transverse momentum of the jet, or equivalently (at NLO precision), on the Q_T of the photon pair. With this cut in place extraction of the signal in the Higgs plus jet mode requires the precise knowledge of both the signal and background distributions in the mid- to high-Q_T region.

To reliably predict the Q_T distribution of Higgs bosons at the LHC, especially in the low to mid Q_T region where the bulk of the rate is, the effects of the multiple soft–gluon emission have to be included. In practice, performing soft gluon resummation within the CSS formalism is equivalent to the determination of the $A^{(n)}$, $B^{(n)}$, and $C^{(n)}$ coefficients and the Y part at some order in α_s. One way to calculate the coefficients is to expand the resummed part in terms of the strong coupling (expanding the exponent an the Wilson

coefficients), and compare the expansion with a fixed order calculation. Luckily, because of its significance, there was much work done on fixed order QCD corrections to Higgs production in the $gg \to HX$ channel. These fixed order QCD corrections are known to substantially increase the rate: by about 70 to 100 percent, depending on the Higgs mass, at $\mathcal{O}(\alpha_s^3)$[20, 21], and by an additional 50 to 70 percent at $\mathcal{O}(\alpha_s^4)$ [22]. It is expected that the calculation of even higher order corrections is important to reliably predict the cross section. In Ref. [23] it was shown that multiple soft–gluon emission dominates the higher order corrections.

2.1 Soft gluon resummation for the $gg \to HX$ channel

Resummed calculations, taking into account the soft–gluon effect, attempted to estimate the size of the non-calculated higher order corrections [23], as well as provide a reliable shape of the Higgs transverse momentum distribution [12, 13]. Our present approach surpasses these by calculating the Q_T distribution while including $\mathcal{O}(\alpha_s^4)$ terms in the Sudakov exponent, using the state of the art matching to the latest fixed order distributions, using a QCD improved gluon-Higgs effective coupling [24], and using an improved non-perturbative function. We utilize the approximation that the object which couples the gluons to the Higgs (the top quark in the SM), is much heavier than the Higgs itself. This approximation is not essential to our calculation and can be released by the calculation of the further Wilson coefficients keeping the relevant masses. The heavy quark approximation in the SM was shown to be reliable within 5 percent for $m_H < 2m_t$ [22, 20, 25], and still reasonable even in the range of $m_H \gtrsim 2m_t$ [23]. It has also been shown that the approximation remains valid for the Q_T distribution in the large Q_T region, provided that $m_H < m_t$ and $Q_T < m_t$ [26]. In this work we assume that the approximation is valid in the whole Q_T region. Unlike the authors of Ref. [23] we do not assume that the QCD corrections to the $gg \to HX$ cross section can be factorized into a multiplicative term in the heavy quark limit in all orders of α_s. We can release this approximation because the CSS formalism, by definition, systematically incorporates higher order fixed order corrections via the definition of the Sudakov exponent and the Wilson coefficients as perturbative expansions [5, 6].

Multiple soft–gluon emission affects the $gg \to HX$ cross section when the transverse momentum of the Higgs is low, while for high transverse momenta the hard gluon radiation is dominant. Thus, using the CSS formalism we resum large logs of the type $\ln(Q/Q_T)$ in the low Q_T region, and we match the resummed result to the fixed order calculation which is valid for high Q_T [5]. We also include the qg and $q\bar{q}$ subprocesses which, depending on the Higgs mass, together constitute 0 to 10 percent of the total rate [20].

The resummed differential cross section of the Higgs boson production in hadronic collisions is written as

$$\frac{d\sigma(h_1 h_2 \to H^0 X)}{dQ^2\, dy\, dQ_T^2} = \sigma_0 \frac{Q^2}{S} \pi\delta(Q^2 - m_H^2)$$
$$\times \left\{ \frac{1}{(2\pi)^2} \int d^2b\, e^{i\vec{Q}_T\cdot\vec{b}} \widetilde{W}_{gg}(b_*, Q, x_1, x_2, C_{1,2,3}) \right.$$

$$\times \widetilde{W}_{gg}^{\rm NP}(b,Q,x_1,x_2) + Y(Q_T,Q,x_1,x_2,C_4)\Big\}\,. \tag{15}$$

The kinematic variables Q, y, and Q_T are the invariant mass, rapidity, and transverse momentum of the Higgs boson in the laboratory frame. The parton momentum fractions are defined as $x_1 = e^y Q/\sqrt{S}$, and $x_2 = e^{-y} Q/\sqrt{S}$, with $\sqrt{S}$ being the center–of–mass (CM) energy of the hadrons h_1 and h_2. The lowest order cross section, with the QCD corrected effective coupling of the Higgs boson to gluons is

$$\sigma_0 = \kappa_\phi(Q) \frac{\sqrt{2} G_F \alpha_s^2(Q^2)}{576\pi}, \tag{16}$$

where G_F is the Fermi constant and κ_ϕ is defined in Ref. [23]. The renormalization group invariant kernel of the Fourier integral $\widetilde{W}_{gg}$ and the regular terms $Y(Q_T,Q,x_1,x_2,C_4)$ (together with the variables b_* and C_1 to C_4) are defined in Ref. [13]. In addition to Ref. [13] we use the process independent coefficient

$$A^{(2)} = C_A \left[\left(\frac{67}{36} - \frac{\pi^2}{12} \right) N_C - \frac{5}{18} N_f \right], \tag{17}$$

in the expansion of the A function ($N_C = 3$ the number of colors and $N_f = 5$ the number of active quark flavors).

2.2 Some numerical results

The resummation formula is coded in the ResBos Monte Carlo event generator [5, 6], which uses the following electroweak input parameters [27]: $G_F = 1.16639 \times 10^{-5}$ GeV^{-2}, $\mathrm{m_Z} = 91.187$ GeV, $\mathrm{m_W} = 80.36$ GeV. The NLO expressions for the running electromagnetic and strong couplings $\alpha(\mu)$ and $\alpha_S(\mu)$ are used, as well as the NLO parton distribution function set CTEQ4M (defined in the modified minimal subtraction, $\overline{MS}$, scheme). The renormalization and factorization scales are set equal to the Higgs invariant mass. In the choice of the non-perturbative parameters we follow Ref. [28]. Since we are not concerned with the decays of Higgs bosons in this work, we do not impose any kinematic cuts.

Fig. 4 displays production cross sections at the LHC, calculated in the SM as the function of the Higgs mass. Our $\mathcal{O}(\alpha_s^3)$ curve agrees well with the result in Ref. [23]. The ratio of the fixed order $\mathcal{O}(\alpha_s^3)$ (dashed) and the lowest order $\mathcal{O}(\alpha_s^2)$ (dotted) curves varies between 2.35 and 2.00. We note that less than 2 percent of the $\mathcal{O}(\alpha_s^3)$ corrections come from the qg and $q\bar{q}$ initial states for Higgs masses below 200 GeV. The resummed curve is slightly (5 to 6 percent) higher than the $\mathcal{O}(\alpha_s^3)$ one, as expected based on the findings that the CSS formalism preserves the fixed order rate within the error of the matching (which is expected to be higher order) [5]. The resummed rate is close to the $\mathcal{O}(\alpha_s^3)$, because we used the $\mathcal{O}(\alpha_s^3)$ fixed order results to derive the Wilson coefficients which are utilized in our calculation. In Ref. [22] the $\mathcal{O}(\alpha_s^4)$ corrections were utilized to show that in the high Q_T region the $\mathcal{O}(\alpha_s^4)$ to $\mathcal{O}(\alpha_s^3)$ K-factor is nearly constant and is about 1.5 (for CTEQ4M parton distributions). Based on this finding we also plot the $\mathcal{O}(\alpha_s^3)$ curve rescaled by 1.5, to illustrate the size of

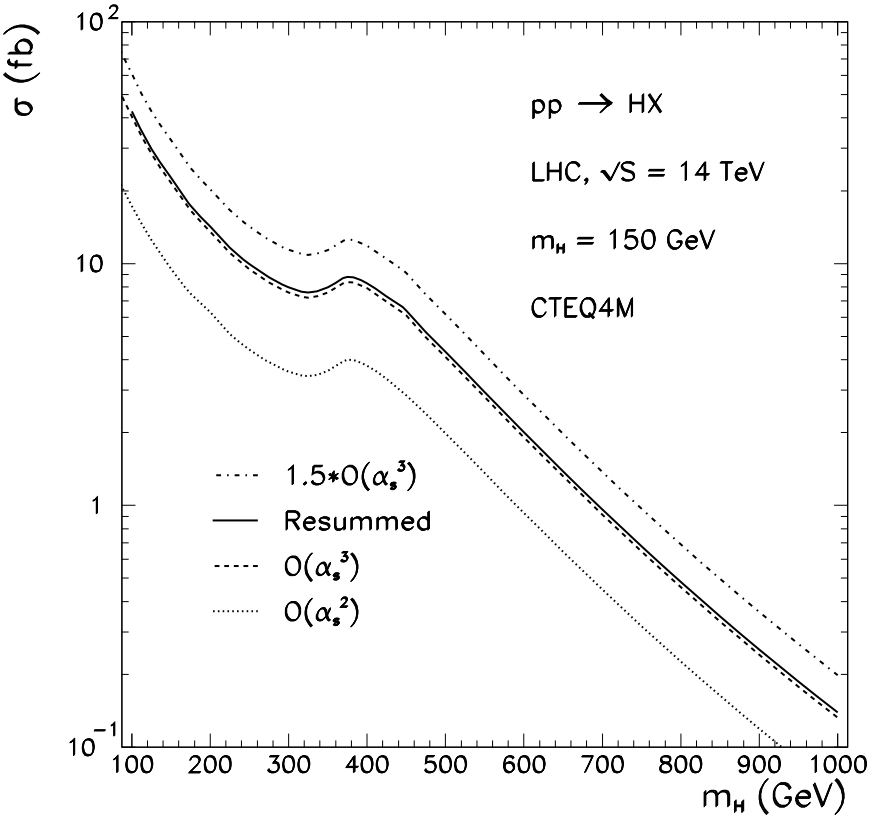

Figure 4: SM Higgs boson production cross sections at the LHC via top quark loop as the function of the Higgs mass, with QCD corrections calculated by soft–gluon resummation (solid), at fixed order $\mathcal{O}(\alpha_s^3)$ (dashed), and without QCD corrections at $\mathcal{O}(\alpha_s^2)$ (dotted). The $\mathcal{O}(\alpha_s^3)$ curve is scaled by 1.5 (dash-dotted, c.f. Ref. [22]) to estimate the $\mathcal{O}(\alpha_s^4)$ result.

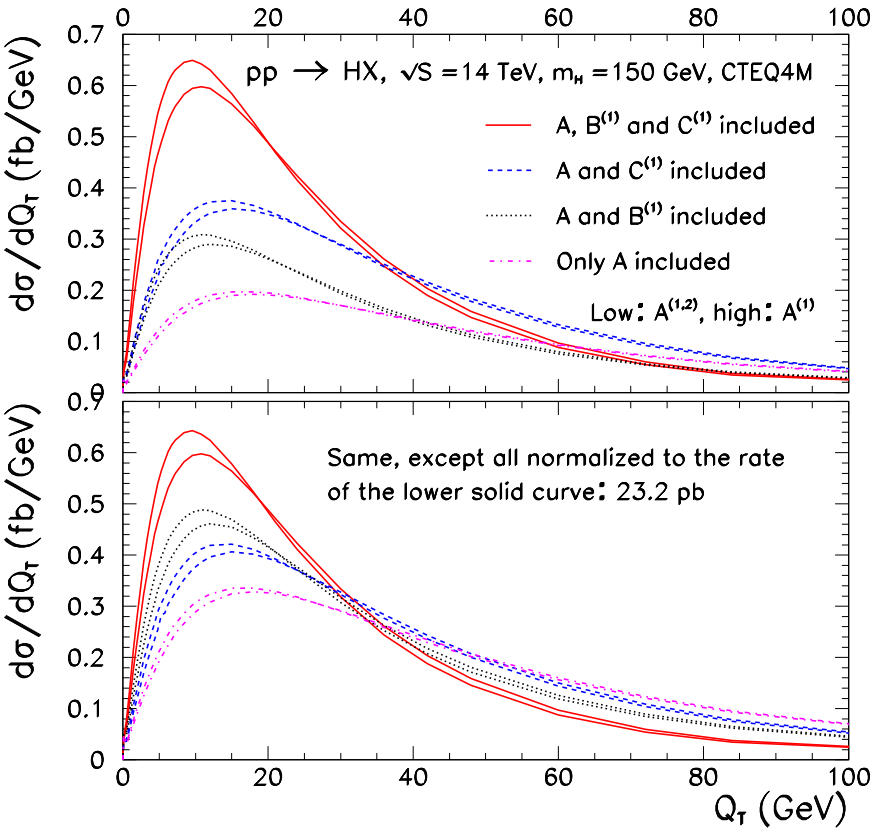

Figure 5: Higgs boson transverse momentum distributions at the LHC, illustrating the effect of various contributions of the CSS formalism. Among the pair of curves the ones which peak lower are calculated by using $A^{(1,2)}$ and the others by $A^{(1)}$. Additionally, the solid curves include $B^{(1)}$ and $C^{(1)}$, the dashed ones $C^{(1)}$, and the dotted ones $B^{(1)}$. The dot-dashed curves only include A coefficients. The lower portion of the figure shows the same curves normalized to the area under the lower peaking solid curve, to compare the changes in the shape.

the $\mathcal{O}(\alpha_s^4)$ corrections and to establish the normalization of our resummed calculation among the fixed order results.

Fig. 5 illustrates the effect of the various contributions of the CSS formalism on the Higgs boson transverse momentum distribution. The lower peaking curves, drawn by the same type line, contain the coefficients $A^{(1,2)}$. The others lack the $A^{(2)}$ coefficient. Comparison of pairs of curves shows that the log multiplied by the $A^{(2)}$ coefficient increases the rate by about 10% around the peak, and decreases it in the mid-Q_T region. The figure also shows that exclusion of the $B^{(1)}$ term leads to about 40% decrease around the peak, and an increase away from it. Finally, the exclusion of the $C^{(1)}$ coefficient decreases the overall rate by about a factor of 2, coupled with some shape change similar to the $B^{(1)}$ case.

Fig. 6 displays transverse momentum distributions of Higgs bosons produced at the LHC. The Q_T distribution is calculated under several different assumptions for the non-perturbative sector of the CSS formalism, in order to span the range of scatter of these different predictions. In Fig. 6a the (solid) curve using the result of the latest 3-parameter fit for the non-perturbative function [28] is shown. (The actual values of the parameters used are: $g_1 = 0.15$ GeV^2, $g_2 = (C_F/C_A) * 0.48$ GeV^2, and $g_3 = -0.58$ GeV^{-1}.) Also shown the (dashed) curve using the result of the latest 3-parameter fit of Ref. [28]. (The values were used are: $g_1 = 0.24$ GeV^2, and $g_2 = (C_F/C_A) * 0.34$ GeV^2.) We plotted the (dotted) curve using the previous 3-parameter fit of Ref. [29], as well. In the lower portion of the figure we show the ratios of the different curves to the solid curve. From this we conclude that the three different parameterizations differ by about 5 percent, at most, in the relevant Q_T region. At $Q_T = 10$ GeV, in the region of the peak of the distribution, the difference is about 2 percent.

In Fig. 6b the solid curve is the same as in Fig. 6a. In this figure results using $g_2 = (C_F/C_A) * 0.33$ GeV^2, and $g_2 = (C_F/C_A) * 0.69$ GeV^2 values are plotted (dashed). These g_2 values are 3 σ deviations from the central value $g_2 = (C_F/C_A) * 0.48$ GeV^2 of the new 3-parameter fit. Also shown a curve with $g_2 = 0.48$ GeV^2, where the assumption that the non-perturbative parameter g_2 scales by C_A/C_F for the gluonic initial state was not utilized. The lower portion of the figure shows that the ratios of the various curves to the solid curve do not deviate from 1 significantly except in the very low Q_T (< 5 GeV) region.

Acknowledgments

We thank the organizers of the les Houches workshop for their hospitality. We are indebted for the CTEQ Collaboration for many invaluable discussions and W. Sakumoto for the CDF results. C.B. thanks M. Spira, and C.-P. Yuan for discussions. This work was supported in part by the DOE under grant DE-FG-03-94ER40833.

References

[1] J.C. Collins and D.E. Soper, Phys. Rev. Lett. **48**, 655 (1982); Nucl. Phys. **B193**, 381 (1981), **B213**, 545(E) (1983).

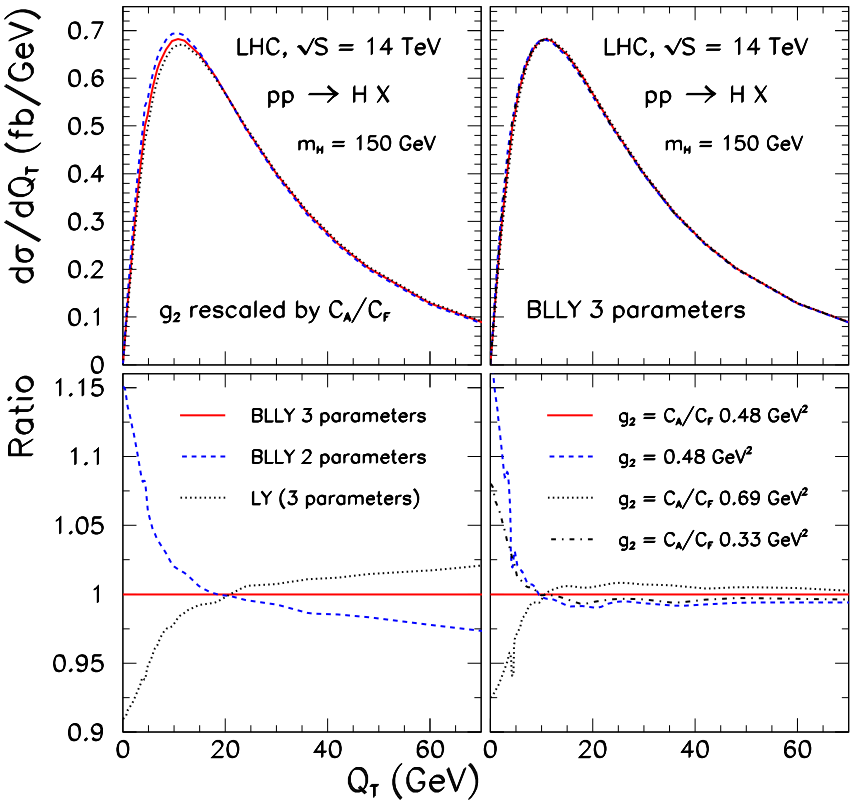

Figure 6: Higgs boson transverse momentum distributions at the LHC, displaying uncertainties arising from the non-perturbative sector of the CSS formalism. a) The solid curve is calculated using the latest 3-parameter fit of the non-perturbative function [28]. The dashed curve uses the new 2-parameter fit [28], and the dotted curve the previous 3-parameter fit [29]. The lower portion shows the ratio of the dashed and the dotted curves to the solid one. b) The solid curve uses the nominal result of the new 3-parameter fit, and the dashed ones are calculated with g_2 parameters deviating by 3 σ from the central value. Also shown in dotted the curve which does not re-scale the g_2 parameter by C_A/C_F. The lower plot shows the ratios with respect to the solid line.

[2] J.C. Collins and D.E. Soper, Nucl. Phys. **B197**, 446 (1982);

[3] J.C. Collins, D.E. Soper and G. Sterman, Nucl. Phys. **B250**, 199 (1985).

[4] The e^+e^- transverse momentum distribution plot is taken from the web-page of the CDF Electroweak Group: http://www-cdf.fnal.gov/physics/ewk/ptz.html

[5] C. Balázs and C.P. Yuan, Phys. Rev. **D56**, 5558 (1997) hep-ph/9704258.

[6] C. Balázs, PhD thesis, Michigan State University (1999) hep-ph/9906422.

[7] P.B. Arnold and R.P. Kauffman, Nucl. Phys. **B349**, 381 (1991).

[8] G. Parisi and R. Petronzio, Nucl. Phys. **B154**, 427 (1979).

[9] R.K. Ellis and S. Veseli, Nucl. Phys. **B511**, 649 (1998) hep-ph/9706526.

[10] C. Balázs, E.L. Berger, S. Mrenna and C.P. Yuan, Phys. Rev. **D57**, 6934 (1998) hep-ph/9712471.

[11] C. Balázs and C.P. Yuan, Phys. Rev. **D59**, 114007 (1999) hep-ph/9810319.

[12] I. Hinchliffe and S.F. Novaes, Phys. Rev. **D38**, 3475 (1988).
R.P. Kauffman, Phys. Rev. **D44**, 1415 (1991); Phys. Rev. **D45**, 1512 (1992);
C. Kao, Phys. Lett. **B328**, 420 (1994) hep-ph/9310206.

[13] C.P. Yuan, Phys. Lett. **B283**, 395 (1992).

[14] C. Balázs and C.P. Yuan, in preparation.

[15] M. Begel, Ph.D thesis, University of Rochester (1999).

[16] P. Nadolsky, D.R. Stump and C.P. Yuan, hep-ph/9906280.

[17] M. Spira, hep-ph/9711394.

[18] ATLAS Collaboration, Technical Proposal,
CERN/LHC/94-43 LHCC/P2 (1994);
CMS Collaboration, Technical Proposal,
CERN/LHC/94-43 LHCC/P1 (1994);
ATLAS Collaboration, Calorimeter Performance,
CERN/LHC/96-40 (1996);
CMS Collaboration, Technical Design Report,
CERN/LHCC/97-33 (1997).

[19] S. Abdullin, M. Dubinin, V. Ilyin, D. Kovalenko, V. Savrin, N. Stepanov, Phys. Lett. **B431**, 410 (1998).

[20] D. Graudenz, M. Spira and P.M. Zerwas, *Phys. Rev. Lett.* **70**, 1372 (1993);

M. Spira, A. Djouadi, D. Graudenz and P.M. Zerwas, *Phys. Lett.* **B 318**, 347 (1993); *Nucl. Phys.* **B 453**, 17 (1995).

[21] A. Djouadi, M. Spira and P.M. Zerwas, *Phys. Lett.* **B 264**, 440 (1991);

S. Dawson, *Nucl. Phys.* **B 359**, 283 (1991);

R.P. Kauffman and W. Schaffer, Phys. Rev. **D49**, 551 (1995);

S. Dawson and R.P. Kauffman, Phys. Rev. **D47**, 1264 (1994).

[22] D. de Florian, M. Grazzini and Z. Kunszt, Phys. Rev. Lett. **82**, 5209 (1999) hep-ph/9902483.

[23] M. Kramer, E. Laenen and M. Spira, Nucl. Phys. **B511**, 523 (1998) hep-ph/9611272.

[24] B.A. Kniehl and M. Spira, Z. Phys. **C69**, 77 (1995) hep-ph/9505225.

[25] Z. Kunszt, S. Moretti and W.J. Stirling, Z. Phys. **C74**, 479 (1997) hep-ph/9611397.

[26] U. Baur and E.W. Glover, Nucl. Phys. **B339**, 38 (1990).

[27] Particle Data Group (C. Caso *et al.*), *The European Physical Journal* **C 3**, 1 (1998).

[28] F. Landry, R. Brock, G. Ladinsky and C.P. Yuan, hep-ph/9905391.

[29] G.A. Ladinsky and C.P. Yuan, Phys. Rev. **D50**, 4239 (1994) hep-ph/9311341.